Chinese Chemical Letters 33 (2022) 973–978

Contents lists available at ScienceDirect

Chinese Chemical Letters

journal homepage: www.elsevier.com/locate/cclet

Design and syntheses of functionalized copper-based MOFs and its adsorption behavior for Pb(II)

Jingping Zhong, Jian Zhou, Minsi Xiao, Jun Liu, Jili Shen, Juan Liu, Sili Ren*

Jiangxi Key Laboratory of Mining Engineering, School of Resources and Environmental Engineering, Jiangxi University of Science and Technology, Ganzhou 341000, China

ARTICLE INFO

Article history:
Received 23 February 2021
Revised 7 June 2021
Accepted 14 July 2021
Available online 24 August 2021

Keywords:
MOFs
Adsorption
Cu(II) ions
Pb(II) ions
Ion exchange
Coordination

ABSTRACT

A novel copper-based MOFs adsorbent (Cu-BTC-Th) was prepared using an one-step method by introducing a new organic ligand of 4-thioureidobenzoicacid (Th) with active groups for selectively adsorbing Pb(II) from aqueous solutions. The chemical composition and structure of the prepared MOFs materials were characterized by scanning electron microscope (SEM), X-ray diffraction (XRD), fourier transform infrared spectroscopy (FTIR), X-ray photoelectron spectroscopy (XPS), Brunner–Emmet–Teller (BET) analysis, and zeta potential measurements. The adsorption capability of the prepared Cu-MOFs was significantly enhanced by introducing the new organic ligand of Th in the materials. The maximum adsorption capacity of the Cu-BTC-Th for Pb(II) attains 732.86 mg/g under the optimal conditions. In addition, the adsorption kinetics and adsorption isotherm analysis showed that the adsorption process followed the *pseudo*-second-order kinetic model and Langmuir adsorption model, indicating that the adsorption of Pb(II) by Cu-BTC-Th was a monolayer chemisorption. The adsorption mechanism of Cu-BTC-Th for Pb(II) was discussed and revealed. On one hand, the adsorption of Pb(II) is mainly through ion exchange with the Cu(II). On the other hand, the $-NH_2$ and $-C=S$ functional groups introduced in the Cu-BTC-Th materials have stronger coordination ability with the Pb(II) ions to enhance the adsorption capability.

Lead is one of the earliest metals used by human beings, which has good flexibility and ductility. It plays a vital role in numerous industrial production and daily routine, such as storage battery, medical apparatus and instruments, building materials, dyes, alloys. However, in the process of industrial application, a considerable amount of lead-containing wastewater is produced, causing environmental pollution [1,2]. Lead mainly exists in water in the form of Pb(II), which can poison the nervous system and cardiovascular system after entering the human body, and 95% of lead is deposited in the skeletal system in the form of phosphate. According to the research reports, entering the human body to 5 mg/kg can lead to death [3,4]. Hence, it is particularly important to remove lead ions from the industrial wastewater.

Treatment methods for lead-containing wastewater include adsorption, chemical precipitation, electrolytic, membrane separation, ion exchange, and biological methods [5]. The adsorption method has always attracted much attention due to its wide range of material sources, simple operation and low cost. The commonly used adsorbents include the activated carbon [6,7], mineral materials [8,9], chitosan [10,11], lignin [12,13], fly ash [14,15], carbon-based materials [16,17] and silica [18,19]. However, the common problems of small pore size, low specific surface area, and incomplete pore arrangement restrict their application. As a novel adsorbent, metal organic frameworks (MOFs) has progressed quickly in late years. MOFs is an organic-inorganic hybrid porous material with three-dimensional periodic grid configuration shaping by self-assembly of metal ions or metal clusters with organic ligands. It has the advantages of high porosity and specific surface area, regular spatial network structure and strong controllability of pore size [20]. Therefore, compared with the common adsorbents mentioned above, MOFs usually has higher adsorption capacity for metal ions. For example, Hasankola *et al*. synthesized Cu-based and Zn-based MOFs using the trimesic acid (BTC) linker. The adsorption capacities of the prepared Cu-BTC and Zn-BTC for Pb(II) ions reached 333 mg/g and 312 mg/g, respectively [21]. Bakhtiari and Azizian prepared a nanoporous metal organic framework (MOF-5), which was employed to adsorb the copper ions with an adsorption capacity about 290 mg/g [22].

However, considerable MOFs adsorbents have low selectivity and adsorption capacity by reason of lacking active functional groups, which limits their wide application. Therefore, besides of the material porosity and specific surface area, the functional

* Corresponding author.
E-mail address: sili_ren@163.com (S. Ren).

https://doi.org/10.1016/j.cclet.2021.07.040
1001-8417/

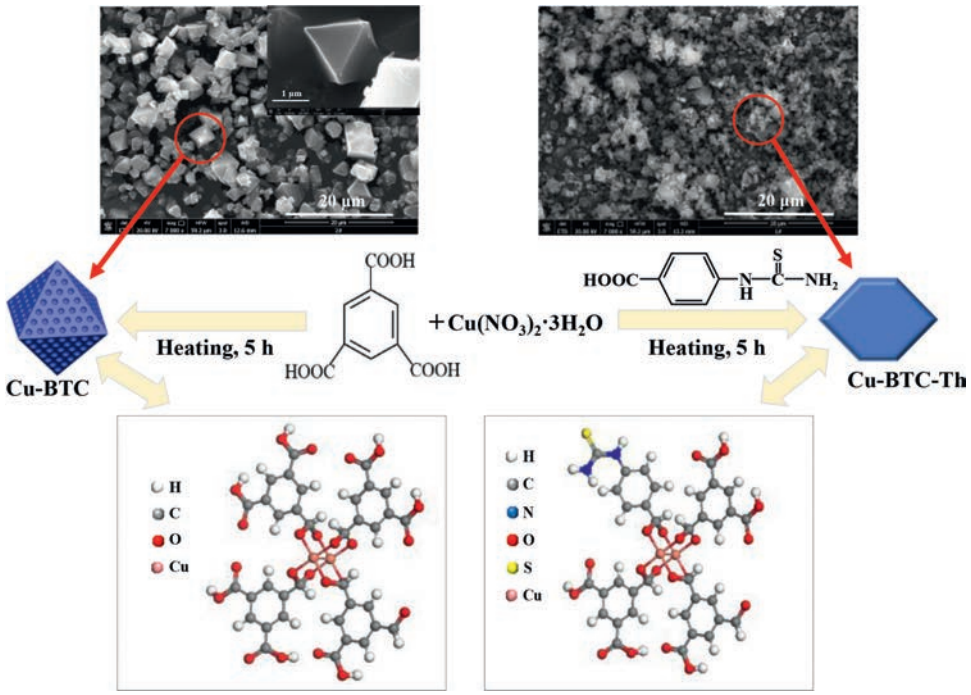

Fig. 1. Schematic presentation of the preparation of Cu-BTC-Th composite and the SEM image of the prepared MOFs.

groups contained in MOFs must be considered to enhance the adsorption performance of the materials. Post-modification method is often used to introduce active functional groups to improve the adsorption capacity and selectivity of the adsorbents. For instance, a Cr-based MOFs (MIL-101) was converted with ethylenediamine (ED) to form amino-functionalized adsorbent (ED-MIL-101). The result revealed that the adsorption capacity of ED-MIL-101 for Pb(II) ions was greatly improved, which was more than five times that of MIL-101 (81.09 mg/g) [23]. Although such a modification is effective, the modification process is too complex. Abdelhameed [24] *et al.* prepared a new type of absorbent (MIL-125-HQ) by modifying the Ti-based metal organic framework (NH_2-MIL-125) with bis-quinoline Mannich base, and its maximum adsorption capacity for Pb(II) is 262.1 mg/g. Zhao [25] *et al.* used $ZrCl_4$, 2-aminoterephthalate and 1,8-dihydroxyanthraquinone to prepare a functionalized adsorbent (MOFs-DHAQ), which has an adsorption capacity of 213.3 mg/g for Pb(II).

As discussed above, we believe that it is a direct and effective way to prepare MOFs by introducing ligands with active functional groups during the preparation process, which can not only simplify the preparation process, but also enhance the adsorption ability and selectivity. On the basis of the theory of hard and soft acid-base (HSAB) [26], sulfur-containing ligands can form stable complexes with Pb(II). 4-Thioureidobenzoicacid (Th) is rich in thionic groups and has not been used in the preparation of MOFs. In this study, using copper nitrate trihydrate as the metal source, and trimesic acid and Th as the organic ligands, a novel MOFs adsorbent (Cu-BTC-Th) was synthesized by a one-step method for selectively adsorbing Pb(II) from aqueous solutions. Effect of the Th introduction on the adsorption performance of the Cu-BTC-Th material was systematically studied. The adsorption conditions were optimized. In addition, the adsorption kinetics and isotherm were studied to reveal the adsorption mechanism.

The preparation process of the copper-based MOFs (Cu-BTC and Cu-BTC-Th) is illustrated in Fig. 1. The preparation details was given in Supporting information. The crystallization of the prepared Cu-BTC and Cu-BTC-Th materials was characterized by the XRD analysis and the consequences are shown in Fig. S1a (Supporting information). It can be seen that several diffraction peaks in the range of $2\theta = 5°\sim40°$ are appeared for the Cu-BTC, which are consistent with those reported in the literature [27,28], indicating that Cu-BTC with crystalline phase has been successfully synthesized. Compared with the Cu-BTC, the intensity of corresponding diffraction peaks for the Cu-BTC-Th is obviously reduced, reflecting that the addition of Th makes the crystallinity of Cu-BTC-Th slightly reduced. Nevertheless, the position of diffraction peaks does not change, indicating that the crystal structure of the Cu-BTC-Th remains unchanged.

In order to confirm whether the new ligand of Th has been introduced in the prepared MOFs, infrared characterization was performed and the results are shown in Fig. S1b (Supporting information). The peak at 1567 cm^{-1} is attribute to the stretching vibration of benzene ring skeleton C=C bond in BTC [29]. Peaks at 1618.98 and 1620.18 cm^{-1} are related to the asymmetric stretching vibration of the O=C−O, while the peaks at 1443 and 1373 cm^{-1} was assigned to the symmetrical stretching vibration of the O=C−O [29,30]. As to the spectrum of Cu-BTC-Th, new peaks at 1249, 1263 and 3415 cm^{-1} appeared, which are designated to the C−N stretching vibration, C=S stretching vibration, and the antisymmetric stretching vibration of the benzene ring, respectively [31,32]. These findings manifest that the ligand of Th has been successfully introduced in the Cu-BTC-Th composites.

Scanning electron microscope (SEM) is an important tool to analyze the surface morphology in the field of materials science. In order to observe the influence of the introduction of new monomers on the morphology of the prepared MOF materials, SEM characterization was performed. As shown in Fig. 1 and Fig. S2a (Supporting information), the Cu-BTC material has a regular octahedral structure, which is consistent with that reported in the literature [33]. In contrast, the microstructure of Cu-BTC-Th changed slightly and the crystallinity decreased (Fig. S2b in Supporting information). Such a finding is consistent with that of the X-ray diffraction (XRD) characterization (Fig. S1a). It has been clear that the Cu-BTC is formed by the connection of the dimeric copper and the H_3BTC, in which the Cu(II) are connected by bond force, and the axial direction is very weak water molecular force, thus form-

ing the primary unit of Cu-BTC. The organic ligands combine these primary units to form an open three-dimensional octahedral structure system [34,35]. Introduction of new monomer of the Th partially destroys the crystal structure and changes the crystal shape to a certain extent. The EDS spectrum (Figs. S2c and d in Supporting information) demonstated the existence of C, N, O, S and Cu in the Cu-BTC-Th composite, and the atomic percents are 47.74%, 6.32%, 36.44%, 1.12% and 8.38%, respectively. The existence of N and S further confirmed that the ligand of Th has been introduced in the prepared Cu-BTC-Th composite.

The specific surface area and pore structure parameters of Cu-BTC and Cu-BTC-Th were characterized by BET analysis. The N_2 adsorption-desorption isotherms is shown in Fig. S3a (Supporting information). According to the IUPAC classification, the isotherms of Cu-BTC and Cu-BTC-Th can be categorized as type IV isotherm with a type H4 hysteresis loop appearing in the range of 0.45 to 1.0, implying that the prepared MOF material has a representative mesoporous structure [36,37]. Table S1 (Supporting information) shows the specific surface area and pore structure parameters of Cu-BTC and Cu-BTC-Th materials. Compared with Cu-BTC, the Cu-BTC-Th composite shows a relative lower specific surface area and pore volume, which is due to the change of the porous structure by introducing the Th monomer.

The surface charge of the adsorbent often plays an important role on the interaction behavior with the adsorbate. Fig. S3b (Supporting information) shows the surface zeta potential of Cu-BTC and Cu-BTC-Th in regard to the solution pH values. It is shown that the zeta potentials of both materials decrease as the increase of the solution pH, which is attributed to the enhanced ionization of carboxyl groups at high pH. In addition, the result shows that the surface charge of Cu-BTC-Th becomes slightly more negative. Such finding seems to be inconsistent with the fact that the introduced Th monomer contains amino groups, which usually leads to an increase in zeta potential. It can be understood considering that on the one hand, the content of the Th monomer in the prepared Cu-BTC-Th composite is very low and less than 5%. On the other hand, the introduction of Th ligand destroys the crystallinity of the Cu-BTC, which might result in more free carboxyl groups exposed on the solid surface. As a result, the zeta potential of the Cu-BTC-Th composite slightly decreased than that of the Cu-BTC material.

Effects of the Th ligand introduction and various factors including the pH, adsorbent dosage and temperature on the adsorption performance of the prepared Cu-BTC-Th materials for Pb(II) were systematically studied. For the preparation of Cu-BTC-Th composite, a certain proportion of Th was added into the BTC precursor solution during the preparation process. To study the effect of Th addition amount on the adsorption performance of Cu-BTC-Th for Pb(II) ions, the molar ratios of Th to H_3BTC were set at 1:50, 1:35, 1:25, and 1:20, respectively. As shown in Fig. 2a, the adsorption capacity of Cu-BTC for Pb(II) is about 643.09 mg/g. With the addition and increase of the Th amount, the adsorption capacity increases gradually. As the molar ratio increases to 1:25, the adsorption capacity of Cu-BTC-Th reaches the maximum value of 732.86 mg/g, which is larger than that reported in the most literatures (Table S2 in Supporting information). Such result, on the one hand, is attributed to the enhanced electrostatic attraction between the materials and Pb(II) ions. And more importantly, the introduction of $-NH_2$ and =S groups enhances the coordination of the Cu-MOFs with the Pb(II) ions. However, when the amount of Th exceeds a certain value, the adsorption capacity decreases greatly. This may be due to the fact that too much of Th destroys the material structure and greatly reduces the specific surface area of the materials. Therefore, the Cu-BTC-Th composites used for the rest of adsorption experiments were prepared according to the molar ratio of 1:25 (Th/BTC).

The pH of the Pb(II) solution is an significant factor influencing the adsorption behavior. The effect of the solution pH in the range of 3∼6 on the adsorption of Pb(II) was inspected. As shown in Fig. 2b, the adsorption capacities of both Cu-BTC and Cu-BTC-Th for Pb(II) are enhanced with the growth of the initial solution pH. This is attributed to that on the one hand, the increase of pH leads to the increase of electronegativity of the adsorbents, which is conducive to the adsorption of Pb(II). On the other hand, at lower pH conditions, the carboxyl and amino groups are easily protonated and exist in the form of $-COOH$ and $-NH_3^+$. An increase in pH will promote the hydrolysis of them turning into $-COO^-$ and $-NH_2$, which will enhance their coordination with Pb(II). It should be noted that the adsorption capacity is particularly low at pH 3, which is probably due to the fact that the adsorbent is partially dissolved in water at a very low pH. When the pH is too high (>6), Pb(II) begins to hydrolyze to form $Pb(OH)^+$, $Pb(OH)_2$, $Pb(OH)_3^-$ and other species, which will interfere with the accuracy of the adsorption capacity. Therefore, the adsorption process will be controlled at pH less than 6.

Fig. 2c shows the effect of the adsorbent dosage on the adsorption capacity of Cu-BTC and Cu-BTC-Th for Pb(II). It can be seen that the adsorption capacity decreased gradually with the increase of the adsorbent dosage. This will be well understood considering that with the increase of adsorbent dosage, the quantity of Pb(II) ions is relatively reduced, which makes the adsorption process difficult to reach a saturated adsorption state.

The effect of temperature on the adsorption of Pb(II) was investigated in the range of 25∼45 °C, and the result was shown in Fig. 2d. It is found that the adsorption capacities of the two adsorbents are gradually increased with the growth of temperature from 25 °C to 45 °C, indicating that the increase of temperature is conducive to the adsorption of Pb(II). This is because the growth of temperature accelerates the activity of Pb(II) ions and promotes their diffusion from the liquid phase to the surface of adsorbent, and enhances the probability of collision between the Pb(II) ions and the adsorption sites on the adsorbent surface. In addition, such a result reflects that the adsorption is an endothermic process and the increase of temperature promotes the adsorption of Pb(II) ions.

Adsorption isotherm is an important way to understand the adsorption behavior. The adsorption isotherms of Cu-BTC and Cu-BTC-Th for Pb(II) was studied by using the Langmuir model and Freundlich model, and the results were shown in Fig. S4a (Supporting information) and Table S3 (Supporting information). It was shown that the correlation coefficients value ($R^2 = 0.9769$) for the Langmuir isotherm model is much higher than that ($R^2 = 0.7654$) for the Freundlich isotherm model, indicating that the adsorption process mainly follows the Langmuir adsorption isotherm and the adsorption of Pb(II) on Cu-BTC and Cu-BTC-Th is a monolayer adsorption. On account of the Langmuir model, the theoretical maximum adsorption capacity of Pb(II) on Cu-BTC-Th is determined to be 838.166 mg/g at temperature of 303 K.

The time for adsorption to reach equilibrium is a key parameter for evaluating the adsorption efficiency of materials. Fig. S4b1 (Supporting information) shows the adsorption capacity variation with respect to the adsorption time. The results show that the adsorption rate is fast in the initial stage of adsorption, then gradually increases, and finally reaches equilibrium at 2 h. The variation of adsorption rate with respect to the time are often described by the *pseudo*-first-order and *pseudo*-second-order kinetic models to reveal the adsorption mechanism. The fitting results are shown in Figs. S4b2 and b3 and Table S3 (Supporting information). It was found that the fitting correlation coefficient of R^2 for the *pseudo*-second-order kinetic model is 0.99997, while it is only 0.8764 for the first-order kinetic model. Therefore, the second-order kinetic model is more matching to depict the kinetics of the Pb(II) ad-

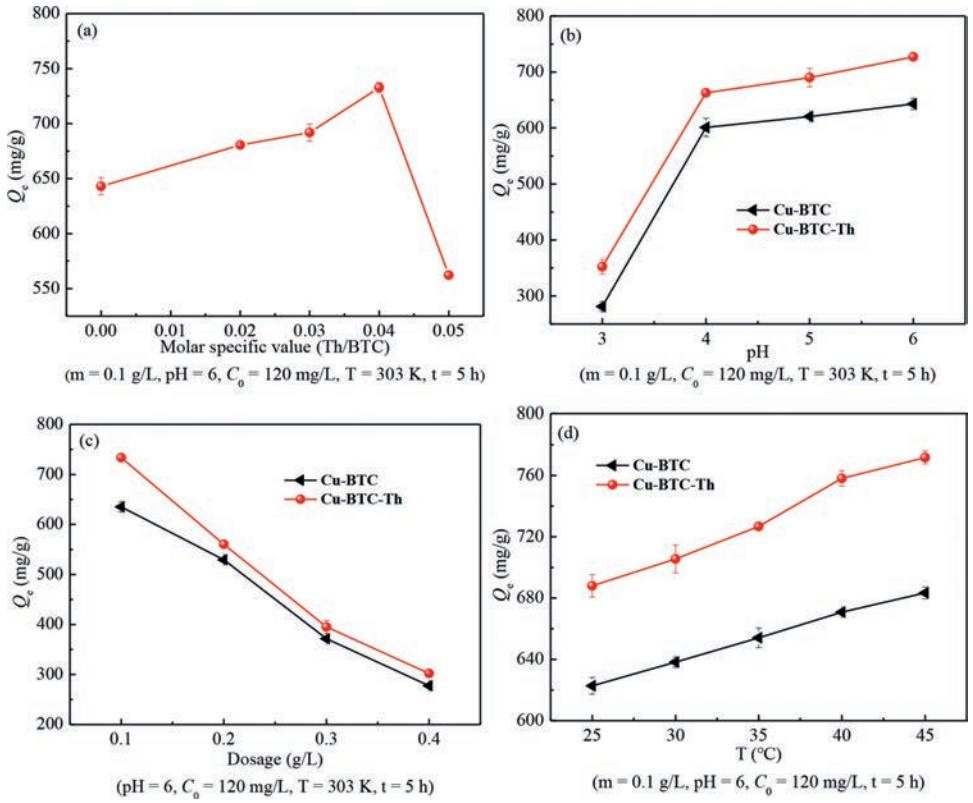

Fig. 2. Effects of Th addition (a) and various factors including the pH (b), adsorbent dosage (c) and temperature (d) on the adsorption performance of the prepared Cu-BTC-Th materials for Pb(II).

sorption, indicating that the adsorption of Pb(II) by Cu-BTC-Th is mainly through chemical adsorption [38].

Selectivity is a crucial factor for the performance of adsorption materials. Heavy metal wastewater generally contains other coexisting metal ions, which may compete with the Pb(II) for the adsorption sites on the adsorbent. Consequently, the adsorption selectivity of Cu-BTC-Th for Pb(II) was studied using Co(II), Cd(II) and Ca(II) as coexisting ions, which have the same concentration as the Pb(II) in the solution. The absorption capacity of Cu-BTC-Th for Pb(II) and the coexisting metal ions were determined as shown in Fig. S5 (Supporting information). It was observed that the existence of calcium ions has a certain competition for the adsorption of Pb(II) ions, which reduces the adsorption capacity of Cu-BTC-Th for Pb(II) ions to a certain extent. In contrast, the effect of Co(II), Cd(II) ions on the adsorption of Pb(II) is very slight. These results indicate that the adsorption of the prepared Cu-BTC-Th for Pb(II) ions has a very good selectivity.

It is believed that the adsorption of Pb(II) by the prepared Cu-BTC-Th is closely correlated with the organic functional groups in the adsorbent materials. The binding behavior between the Pb(II) and various functional groups is the key to the high adsorption performance of the Cu-BTC-Th. To explore the interaction between Cu-BTC-Th and Pb(II), X-ray photoelectron spectroscopy (XPS) was performed. In high-resolution spectrum of Pb 4f (Fig. 3a), the binding energies for Pb $4f_{7/2}$ and $4f_{5/2}$ are appeared at 139.03 eV and 143.9 eV, respectively. For the spectra of O 1s (Fig. 3b), peak at 531.85eV corresponds to the O element in the −COO···Cu group [39]. After adsorbing the Pb(II) ions, the peak position shifts to a low binding energy at 531.42 eV, which is assigned to the −COO···Pb, implying that ions exchange was occurred between Cu(II) and Pb(II) during the adsorption process. Because the electronegativity of Pb(II) is lower than that of Cu(II), the substitution of Pb(II) for Cu(II) relatively increases the electron cloud density of oxygen atoms, so the binding energy shifts to a lower position. To further prove the exchange of Pb(II) with Cu(II), the content of Cu(II) and Pb(II) ions in the solution were measured before and after the adsorption. As shown in Table S4 (Supporting information), the content of Cu(II) in the solution increased from zero to 0.25 mmol/L, which is about 67.6% of the reduction of the Pb(II) ions due to adsorption. These results demonstrated that the adsorption of Pb(II) ions by the Cu-BTC-Th materials is partially through ion exchange.

The N 1s high-resolution XPS spectra are shown in Figs. c1 and c2. Before adsorbing the Pb(II), the N 1s peak is appeared at 399.88 eV representing the H_2N−C(S)−NH− group [40,41]. After adsorbing the Pb(II), the N 1s spectrum is divided into two peaks (Fig. 3c2), in which the peak at 407.02 eV is attributed to the formation of coordination bond of −N···Pb. The coordination of $-NH_2$ groups with Pb(II) induces a ~7.14eV shift toward high binding energy, which was due to the electron donor effect of the lone electron pair of nitrogen atom [42]. In high-resolution spectrum of S 2p (Fig. 3d1-2), to simplify the analysis, only the S $2p_{3/2}$ peak was analyzed [43,44], the S $2p_{3/2}$ peak at around 164.3 eV [45] is related to the S atoms in C=S group. After adsorbing the Pb(II), the spectrum of S 2p changed obviously, demonstrating that the chemical enviorement of S atoms in Cu-BTC-Th-Pb composite changed. The new peak appeared at 167.24 eV is likely derived from S-Pb groups, which has an aout 3 eV shift to the high binding energy due to the coordination with Pb(II). In addition, the peak at 169.94 eV indicates that a very small amount of C=S may be oxidized during the adsorption process. The O 1s, N 1s and S 2p results confirmed that the adsorption process of Cu-BTC-Th for the Pb(II) ions involves the complexation of nitrogen, oxygen and sulfur-containing functional groups with the lead ions.

As discussed above, the adsorption mechanism of the Cu-BTC-Th materials for Pb(II) ions was proposed and illustrated in Fig. 4.

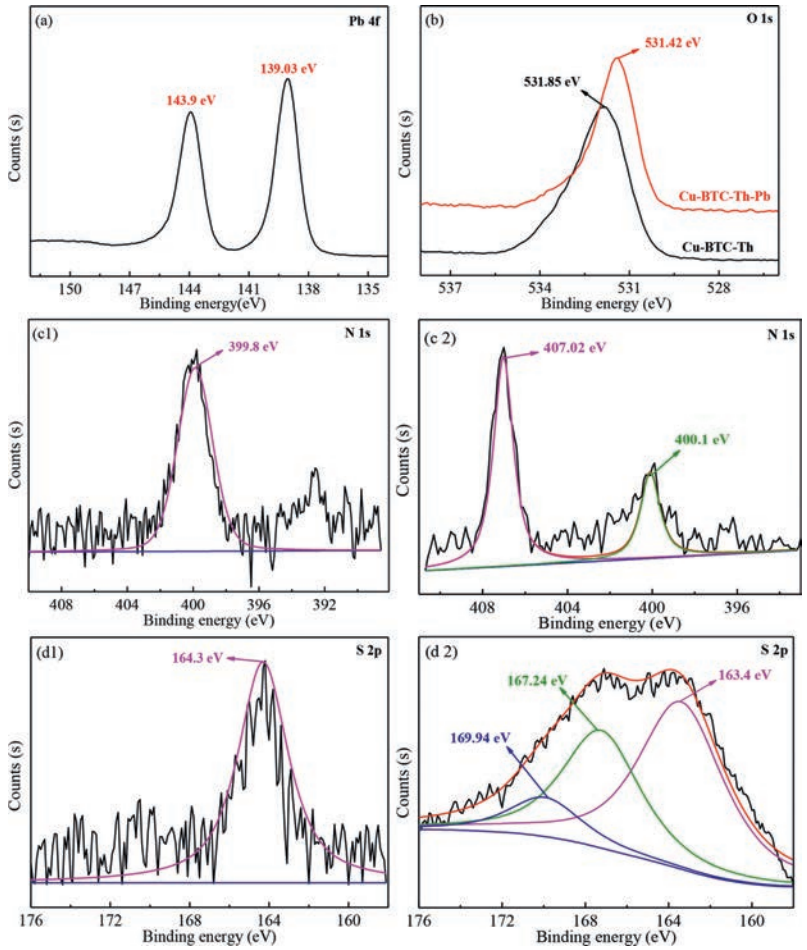

Fig. 3. The high-resolution spectra of Pb 4f (a), O 1s (b), N 1s (c1, c2), S 2p (d1, d2) of Cu-BTC-Th before and after adsorption of Pb(II).

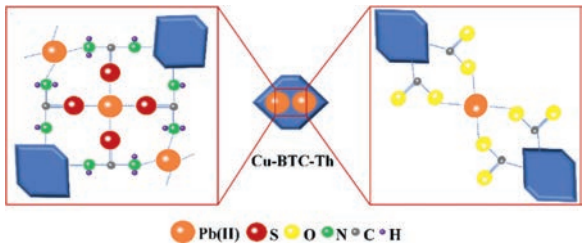

Fig. 4. Schematic of the adsorption mechanism of Pb(II) on Cu-BTC-Th.

At one hand, through ion exchange with the Cu(II) ions, the Pb(II) ions enter into the adsorbent materials to coordinate with carboxyl groups. At the other hand, the $-NH_2$ and $-C{=}S$ functional groups introduced in the Cu-BTC-Th materials have stronger coordination ability with Pb(II) ions. Therefore, the adsorption performance of the prepared Cu-MOFs for Pb(II) ions was significantly enhanced by introducing the new organic ligand of Th in the materials.

The reusability of Cu-BTC-Th material and its preliminary application in processing a real heavy metal ions wastewater were carried out and the results were shown in Fig. S6 and Table S5 (Supporting information).

In summary, a novel copper-based MOFs adsorbent (Cu-BTC-Th) was synthesized by a one-step method using trimesic acid (BTC) and 4-Thioureidobenzoicacid (Th) as the organic ligands for selectively adsorbing Pb(II) from aqueous solutions. It was found that by introducing the new organic ligand of Th in the materials, the adsorption capability of the prepared Cu-MOFs was significantly enhanced. The maximum adsorption capacity of the Cu-BTC-Th for Pb(II) attains 732.86 mg/g under the optimal conditions. More importantly, the materials have high selectivity for the adsorption of Pb(II) ions. The adsorption kinetics and adsorption isotherm analysis showed that the adsorption process followed the *pseudo*-second-order kinetic model and Langmuir adsorption model, indicating that the adsorption of Pb(II) by Cu-BTC-Th was a monolayer chemisorption. The adsorption mechanism of Cu-BTC-Th for Pb(II) was explored. It was revealed that ion exchange with Cu(II) ions is an important way for the Pb(II) adsorption. Moreover, the $-NH_2$ and $-C{=}S$ functional groups introduced in the Cu-BTC-Th materials have stronger coordination ability with the Pb(II) ions to enhance the adsorption capability. These findings indicate that the prepared Cu-BTC-Th material has potential application value in the treatment of Pb(II) heavy metal wastewater.

Declaration of competing interest

The authors declare that they have no known competing financial interests or personal relationships that could have appeared to influence the work reported in this paper.

Acknowledgments

The authors acknowledge the financial support from the National Key Research and Development Program of China (No. 2018YFC1903401), Key Projects of Natural Science Foundation of Jiangxi Province (No. 20202ACBL203009), and "Thousand Talents Plan" of Jiangxi Province (No. Jxsq2018101018).

Supplementary materials

Supplementary material associated with this article can be found, in the online version, at doi:10.1016/j.cclet.2021.07.040.

References

[1] Z. Feng, S. Zhu, G.R.M. Godoi, A.C.S. Samia, D. Scherson, Anal. Chem. 84 (2012) 3764–3770.
[2] Y. Wang, G.Q. Ye, H.H. Chen, et al., J. Mater. Chem. 3 (2015) 15292–15298.
[3] X. Zeng, X. Huo, X.J. Xu, D.L. Liu, W.D. Wu, Sci. Total Environ. 734 (2020) 139286.
[4] H. Toyomaki, J. Yabe, S.M.M. Nakayama, et al., Chemosphere 247 (2020) 125884.
[5] Y.F. Xu, H. Zhang, Q.L. Zeng, J. Anhui Agri. Sci. 42 (2014) 2709–2711.
[6] K.G. Sreejalekshmi, K.A. Krishnan, T.S. Anirudhana, J. Hazard. Mater. 161 (2009) 1506–1513.
[7] S.Z. Mohammadi, H. Hamidian, Z. Moeinadini, J. Ind. Eng. Chem. 20 (2014) 4112–4118.
[8] Y. Song, P. Yuan, P. Du, et al., Appl. Clay. Sci. 186 (2020) 105450.
[9] J. Liu, L.Q. Zeng, S. Liao, et al., Chin. Chem. Lett. 31 (2020) 2849–2853.
[10] X.Y. Li, H.H. Zhou, W.Q. Wu, et al., J. Colloid Interface Sci. 448 (2015) 389–397.
[11] H.Q. Chang, Q.Z. Wang, Z.J. Li, et al., Chin. Chem. Lett. 19 (2020) 1375–1386.
[12] A. Demirbas, J. Hazard. Mater. 109 (2004) 221–226.
[13] M.R. Yakubova, V.P. Ryabchenko, A.A. Stancheva, et al., Chem. Nat. Compd. 31 (1995) 534–535.
[14] F. Miyaji, S. Masuda, Y. Suyama, J. Ceram. Soc. Jpn. 118 (2010) 1062–1066.
[15] Q.H. Wang, J. Yang, Q. Wang, T.J. Wu, J. Hazard. Mater. 162 (2009) 812–818.
[16] N.A. Kabbashi, M.A. Atieh, A. Al-Mamun, et al., J. Environ. Sci. 21 (2009) 539–544.
[17] M.F. Hossain, N. Akther, Y.B. Zhou, Chin. Chem. Lett. 31 (2020) 2525–2538.
[18] H.R. Pouretedal, M. Kazemi, Int. J. Ind. Chem. 3 (2012) 20–27.
[19] W.J. Yang, P. Ding, L. Zhou, et al., Appl. Surf. Sci. 282 (2013) 38–45.
[20] H.C. Zhou, J.R. Long, O.M. Yaghi, Chem. Rev. 112 (2012) 673–674.
[21] Z.S. Hasankola, R. Rahimi, V. Safarifard, Inorg. Chem. Commun. 107 (2019) 107474.
[22] N. Bakhtiari, S. Azizian, J. Mol. Liq. 206 (2015) 114–118.
[23] X.B. Luo, L. Ding, J.M. Luo, J. Chem. Eng. Data 60 (2015) 1732–1743.
[24] R.M. Abdelhameed, R.A. Ismail, M. El-Naggar, et al., Micropor. Mesopor. Mater. 279 (2019) 26–36.
[25] J. Zhao, C. Wang, S. Wang, et al., J. Ind. Eng. Chem. 83 (2019) 111–122.
[26] R.G. Pearson, J. Am. Chem. Soc. 85 (1973) 3533–3539.
[27] K. Schlichte, T. Kratzke, S. Kaskel, Micropor. Mesopor. Mater. 73 (2004) 81–88.
[28] R. Liu, W. Zhang, Y.T. Chen, Y.S. Wang, Colloid Surface A 587 (2020) 124334.
[29] F.R.S. Flávia, L.C.C. Araújo, M.D. Rodrigues, et al., Biomed. Pharmacother. 67 (2013) 707–713.
[30] Q.Y. Li, S. Jiang, S.F. Ji, et al., Ind. Eng. Chem. Res. 53 (2014) 14948–14955.
[31] O. Estévez-Hernández, E. Otazo-Sánchez, J.L.H. Cisneros, et al., Spectrochim. Acta. A 64 (2006) 961–971.
[32] Q.J. Xing, Synthesis, Characterization and Crystal Structure of Bismuth Disulfide Complex[D], Northwest University, 2005.
[33] V. Chevalier, J. Martin, D. Peralta, A. Roussey, F. Tardif, J. Environ. Chem. Eng. 7 (2019) 103131.
[34] N.C. Jeong, B. Samanta, C.Y. Lee, O.K. Farha, J.T. Hupp, J. Am. Chem. Soc. 134 (2012) 51–54.
[35] T. Böhle, F. Mertens, Micropor. Mesopor. Mater 183 (2014) 162–167.
[36] K.S.W. Sing, D.H. Everett, R.A.W. Haul, et al., Pure Appl. Chem. 57 (1985) 603–619.
[37] K.J. Kim, Y.J. Li, P.B. Kreider, et al., Chem. Commun. 49 (2013) 11518–11520.
[38] M.R. Razanajatovo, W.Y. Gao, Y.R. Song, et al., Chin. Chem. Lett. 32 (2021) 2637–2647.
[39] B.J. Zhu, X.Y. Yu, J. Yong, et al., J. Phys. Chem. C 116 (2012) 8601–8607.
[40] A.M. Khattak, Z.A. Ghazi, B. Liang, et al., J. Mater. Chem. A 4 (2016) 16312.
[41] S.W. Zhang, J.X. Li, X.K. Wang, et al., J. Mater. Chem. A 3 (2015) 10119–10126.
[42] R. He, W.M. Li, D.Y. Deng, W.S. Chen, J. Mater. Chem. A 3 (2015) 9789–9798.
[43] T. Grzybek, R. Pietrzak, H. Wachowska, Fuel Process. Technol. 77 (2002) 1–7.
[44] L.L. Ma, Z.H. Qin, L. Zhang, J. Fuel Chem. Technol. 42 (2014) 277–283.
[45] M.L. Pang, H.C. Zeng, Langmuir 26 (2010) 5963–5970.